

Article

# Economic Consequences of Cooling Water Insufficiency in the Thermal Power Sector under Climate Change Scenarios

Qian Zhou <sup>1,2</sup>, Naota Hanasaki <sup>1,\*</sup>  and Shinichiro Fujimori <sup>3,4</sup> 

<sup>1</sup> Center for Global Environmental Research, National Institute for Environmental Studies, Tsukuba 305-8506, Japan; zhou.qian@nies.go.jp

<sup>2</sup> School of Economics and Management, North China Electric Power University, Changping, Beijing 102206, China

<sup>3</sup> Department of Environmental Engineering, Kyoto University, Kyoto 615-8540, Japan; sfujimori@athehost.env.kyoto-u.ac.jp

<sup>4</sup> Center for Social and Environmental Systems Research, National Institute for Environmental Studies, Tsukuba 305-8506, Japan

\* Correspondence: hanasaki@nies.go.jp

Received: 12 September 2018; Accepted: 2 October 2018; Published: 9 October 2018



**Abstract:** Currently, thermal power is the largest source of power in the world. Although the impacts of climate change on cooling water sufficiency in thermal power plants have been extensively assessed globally and regionally, their economic consequences have seldom been evaluated. In this study, the Asia-Pacific Integrated Model Computable General Equilibrium model (AIM/CGE) was used to evaluate the economic consequences of projected future cooling water insufficiency on a global basis, which was simulated using the H08 global hydrological model. This approach enabled us to investigate how the physical impacts of climate change on thermal power generation influence economic activities in regions and industrial sectors. To account for the uncertainty of climate change projections, five global climate models and two representative concentration pathways (RCPs 2.6 and 8.5) were used. The ensemble-mean results showed that the global gross domestic product (GDP) loss in 2070–2095 due to cooling water insufficiency in the thermal power sector was  $-0.21\%$  ( $-0.12\%$ ) in RCP8.5 (RCP2.6). Among the five regions, the largest GDP loss of  $-0.57\%$  ( $-0.27\%$ ) was observed in the Middle East and Africa. Medium-scale losses of  $-0.18\%$  ( $-0.12\%$ ) and  $-0.14\%$  ( $-0.12\%$ ) were found in OECD90 (the member countries of the Organization for Economic Co-operation and Development as of 1990) and Eastern Europe and the Former Soviet Union, respectively. The smallest losses of  $-0.05\%$  ( $-0.06\%$ ) and  $-0.09\%$  ( $-0.08\%$ ) were found in Latin America and Asia, respectively. The economic impact of cooling water insufficiency was non-negligible and should be considered as one of the threats induced by climate change.

**Keywords:** cooling water shortage; thermal power; economic consequence; climate change

## 1. Introduction

Cooling water is indispensable to thermal power generation, which supplies approximately 80% of the world's electricity [1]. For example, it is estimated that 41% of freshwater withdrawal in the U.S. in 2005 was used for electricity production, mainly for cooling [2]. Likewise, in 2010, it was reported that the water withdrawal for cooling purposes in France and Germany was 22 km<sup>3</sup> and 20 km<sup>3</sup>, respectively [3]. Because water demand is growing in many parts of the world, water competition among sectors (e.g., municipal use, agriculture, and manufacturing) could be aggravated in the future unless effective countermeasures are taken [4]. In particular, climate change will increase the risk of

thermoelectric cooling water shortages, which are primarily accompanied by decreases in low flow and increases in stream temperatures [5,6]. The former imposes physical water constraints due to limited streamflow availability, whereas the latter increases the risk of violating environmental regulations, which prohibit water abstraction under high stream temperature conditions [7].

The impacts of climate change on thermoelectric cooling water insufficiency have been extensively investigated globally. Most studies have been based on global hydrological models, which are capable of simulating streamflow and stream temperature at daily intervals [5,6,8,9]. This approach enables the projection of future cooling water availability at a high spatiotemporal resolution (typically  $0.5^\circ \times 0.5^\circ$  on a daily basis), while taking into account both the effects of decreasing low flow and increasing stream temperatures. Earlier studies estimated that the capacity reduction due to cooling water insufficiency in 2050 would be as much as 7–12%, 2.4–16%, and 1.5–19% globally, in the U.S., and in Europe, respectively [5,6,8–10]. Although physical (i.e., hydrological) aspects have been well simulated, this approach has tended to neglect the socio-economic dynamics (i.e., fixing the cooling water requirements at the base year of simulation). To project cooling water withdrawal and consumption while incorporating socio-economic changes, such as population growth, increased gross domestic product (GDP), technological improvements, and policy implementation for climate change mitigation, several studies have used global economic models [11–13]. Although the aforementioned shortcomings of hydrological models have been resolved, owing to their lack of spatiotemporal detail regarding hydrological processes, their ability to assess cooling water sufficiency (CWS) is restricted.

To tackle this problem, a recent study by Zhou et al. first combined these two approaches [10]. They used the Asia Pacific Integrated Model Computable General Equilibrium model (AIM/CGE) [14] and projected the thermoelectric cooling water requirement of the 21st century, taking the growth in electricity demand and expected technological advances into account. Then, they assessed the availability of streamflow to meet the projected water requirement on a daily basis using the H08 global hydrological model, including water abstraction for the agricultural, manufacturing, and municipal sectors [15,16]. They defined CWS as the ratio of the accumulation of daily water abstraction for the consumptive use for cooling (ACC) to the water requirement for the consumptive use for cooling (RCC) for a specific year. They estimated the CWS for 17 regions at an annual interval during the 21st century for two representative concentration pathway (RCP) scenarios and five global climate models (GCMs).

In this study, the economic consequences of cooling water insufficiency for thermal power plants was investigated globally, based on Zhou et al. [10]. The projected CWS was fed into the AIM/CGE by converting the changes in CWS into changes in the capital productivity of thermoelectric sectors. The key advance made in this study was the quantification of climate change impacts on thermoelectric production and their economic consequences through a two-way coupling of a hydrological model and an economic model (i.e., one way is from the former to the latter as in Zhou et al., whereas another is the opposite approach, as shown in this study). The objective of this study was to answer the following two questions. What are the economic consequences, more specifically, the magnitude of GDP losses, due to the cooling water insufficiency projected by Zhou et al. [10]? Which regions and sectors are more (and less) affected compared to the global mean?

The rest of the paper is organized as follows. The methods are described in Section 2. The results and discussion are presented in Section 3. Finally, the conclusions are presented in Section 4.

## 2. Methods

We estimated the economic consequences of the deterioration of CWS in the thermoelectric sector associated with climate change from 2005 (the baseline year) to 2100. To achieve this goal, we used the H08 global hydrological model [15,16] and the AIM/CGE global economic model [17]. The schematic of the methodology and the data flows between these models are shown in Figure 1. Our study proceeded in three steps. In step 1, we used AIM/CGE to project the RCC globally. The shared socioeconomic pathway 2 (SSP2) scenario and a climate policy compatible with RCP2.6 and RCP8.5 were assumed in the simulations. In step 2, we used H08 to project the accumulation of

daily water abstraction for the consumptive use of cooling (ACC,  $ACC \leq RCC$ ) taking hydrological constraints (i.e., daily streamflow availability) into account. By dividing ACC by RCC, the CWS indicator ( $0 \leq CWS \leq 1$ ) was derived. These processes and results are detailed in Zhou et al. [10]. In step 3, we used the AIM/CGE to estimate the economic consequences of the change in CWS. Here, we assumed that the change in CWS was equivalent to the change in capital productivity in the thermal power sector, which is a key parameter in AIM/CGE. The change in capital productivity resulted in a deterioration in electricity production in the thermoelectric sector. Non-thermal power sectors (e.g., hydropower, photovoltaic, and wind power) were not affected. The simulations were conducted under the same conditions as those in Step 1.

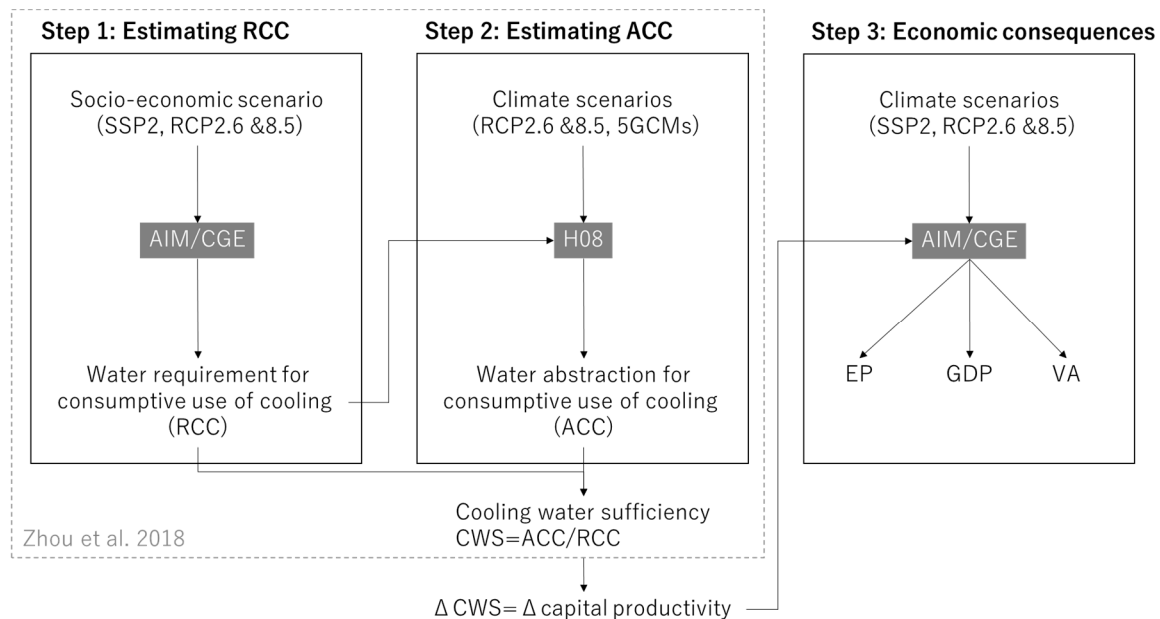


**Figure 1.** Schematic of the models and data flows. AIM/CGE and H08 denote the Asia-Pacific Integrated Model/Computable General Equilibrium (AIM/CGE) and the H08 global hydrological model, respectively. SSP, RCP, GCM, EP, GDP, and VA denote Shared Socioeconomic Pathway, Representative Concentration Pathway, Global Climate Model, Electricity Production, Gross Domestic Production, and Value Added, respectively.

### 2.1. AIM/CGE Model

AIM/CGE is a recursive-dynamic general equilibrium model which is based on the “standard CGE model” [18]. It subdivides the world and industry into 17 regions and 42 sectors (Tables S1 and S2). Details of the model’s structure and mathematical formulas are described in the AIM/CGE basic manual [17].

The structure of electricity production in AIM/CGE is shown in Figure 2. The electricity production industry consists of 11 sectors by fuel type which are combined with a Logit Function. Coal (COL), oil (OIL), natural gas (GAS), nuclear (NUC), geothermal (GEO), advanced biomass-power generation (BIN), waste biomass power (BIO), and other renewable energy power generation (ORN) are thermal power sources that require cooling water. Hydro (HYD), solar photovoltaic (SPV), and wind (WIN) are non-thermal power generation systems. We assumed that the cooling water supply was sufficient for all thermal power plants at the base year. Due to the effects of climate change and the growth in water consumption, CWS will deteriorate over time [10]. The decay in CWS is transferred into a decay in capital productivity in the thermoelectric sector. This reduces the productivity of the thermoelectric sector, which eventually affects all economic activities.

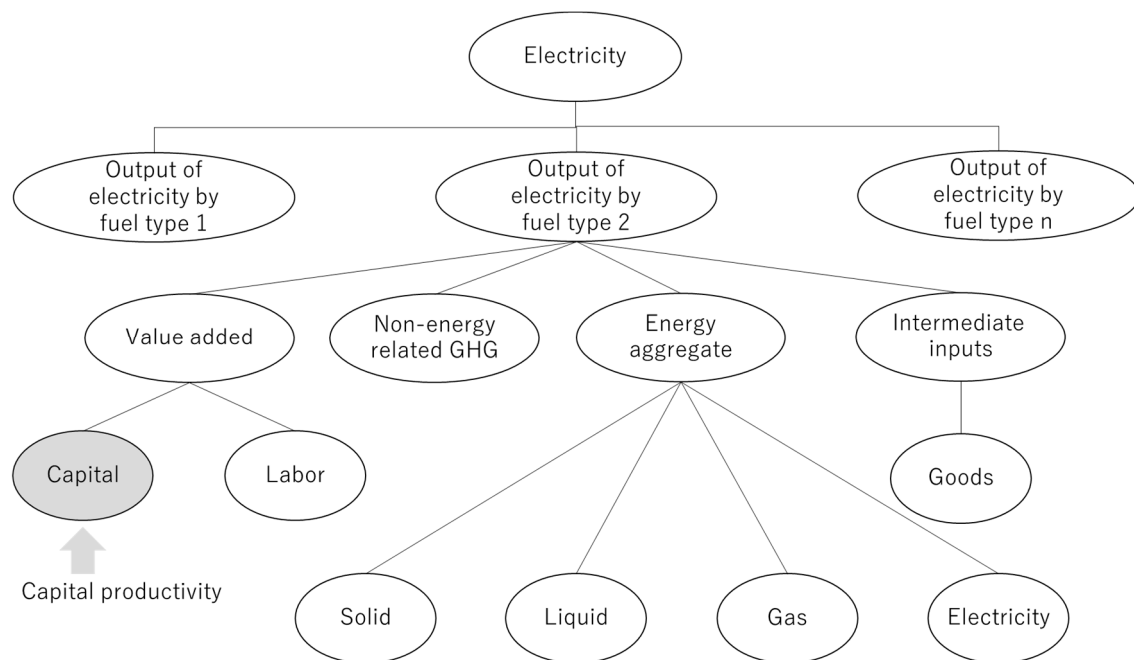


**Figure 2.** The structure of electricity production. Diagonal and straight lines denote the Leontief and logit functions, respectively.

## 2.2. Scenario-Setting and Analysis

We conducted a series of global economic simulations using AIM/CGE. All simulations covered the period from 2005 to 2100. Global economic growth during the period was compatible with the SSP2 socioeconomic conditions [19]. The simulations were repeated three times with different assumptions. The first was a world in which a cooling water shortage had no impact on economic activities (no climate change impacts; NoCC). The second and third were worlds in which the cooling water shortages of RCP2.6 and RCP8.5 influenced economic activities. The projected cooling water insufficiency (Steps 1–2 in Figure 1) was transferred into a decay in the factor of productivity of AIM/CGE. To quantify the uncertainties in climate projections by GCMs, we performed all simulations five times using the CWS results of five individual GCMs, then calculated the mean changes for both RCP2.6 and RCP8.5.

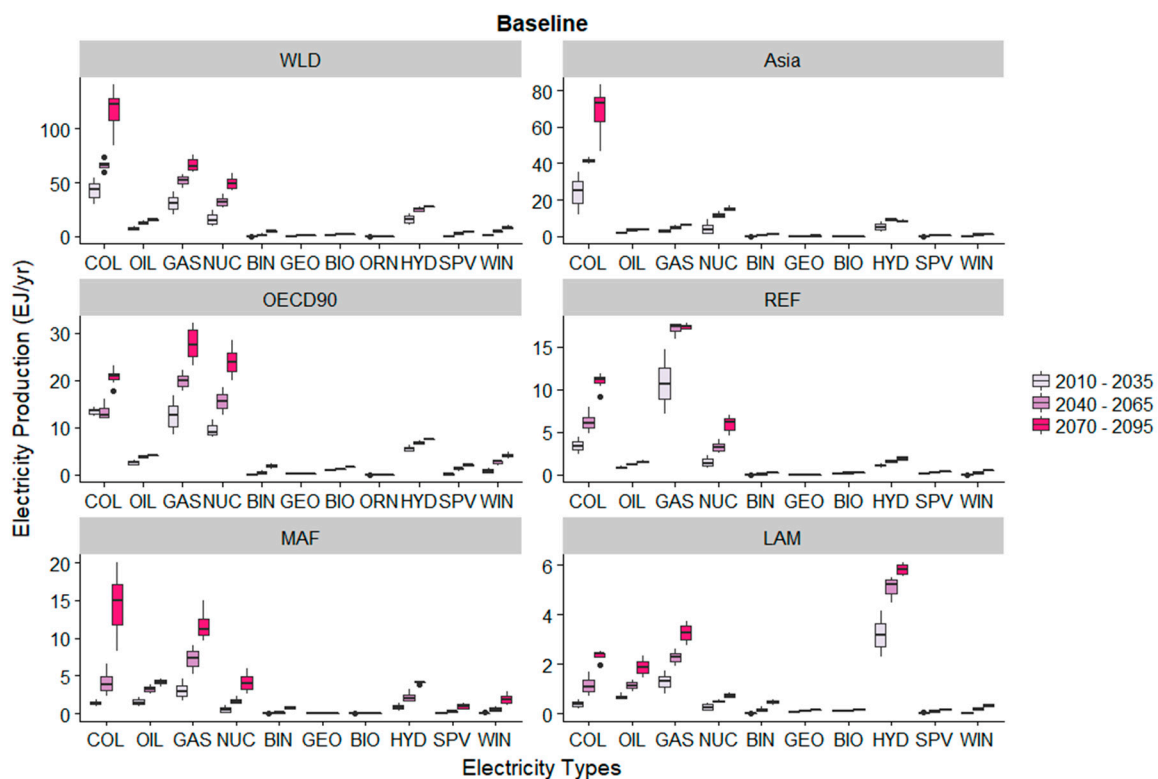
All simulation results for the 17 regions and 42 sectors were obtained at annual intervals. To better interpret the results, we aggregated the results as follows. First, we aggregated time into three periods: 2010–2035, 2040–2065, and 2070–2095. Second, we aggregated the 17 regions (Table S1) into five large regions: Asia, the Middle East and Africa (MAF), Latin America (LAM), the member countries of the Organization for Economic Co-operation and Development as of 1990 (OECD90), and Eastern Europe and the Former Soviet Union (REF). Finally, we aggregated the 42 sectors (Table S2) into six large sectors: agriculture (AGR), manufacturing and construction (MAN), energy extraction (ENE), power (PWR), transport and communications (TRS), and service (SER).

## 3. Results and Discussion

### 3.1. Climate Change Impacts on Electricity Production

Figure 3 shows a boxplot of electricity production for the NoCC run. It shows the results for the world (WLD) and five regions for the eight thermal and three non-thermal power sources for 2010–2035, 2040–2065, and 2070–2095. Because thermal power production was unaffected by climate change impacts (i.e., cooling water shortage) in the NoCC run, the results were used as a reference in this study. The range between the lower and the upper whisker in each boxplot shows the annual variations within each simulation period (25 years). Globally, COL (median in 2070–2095: 123 EJ yr<sup>-1</sup>),

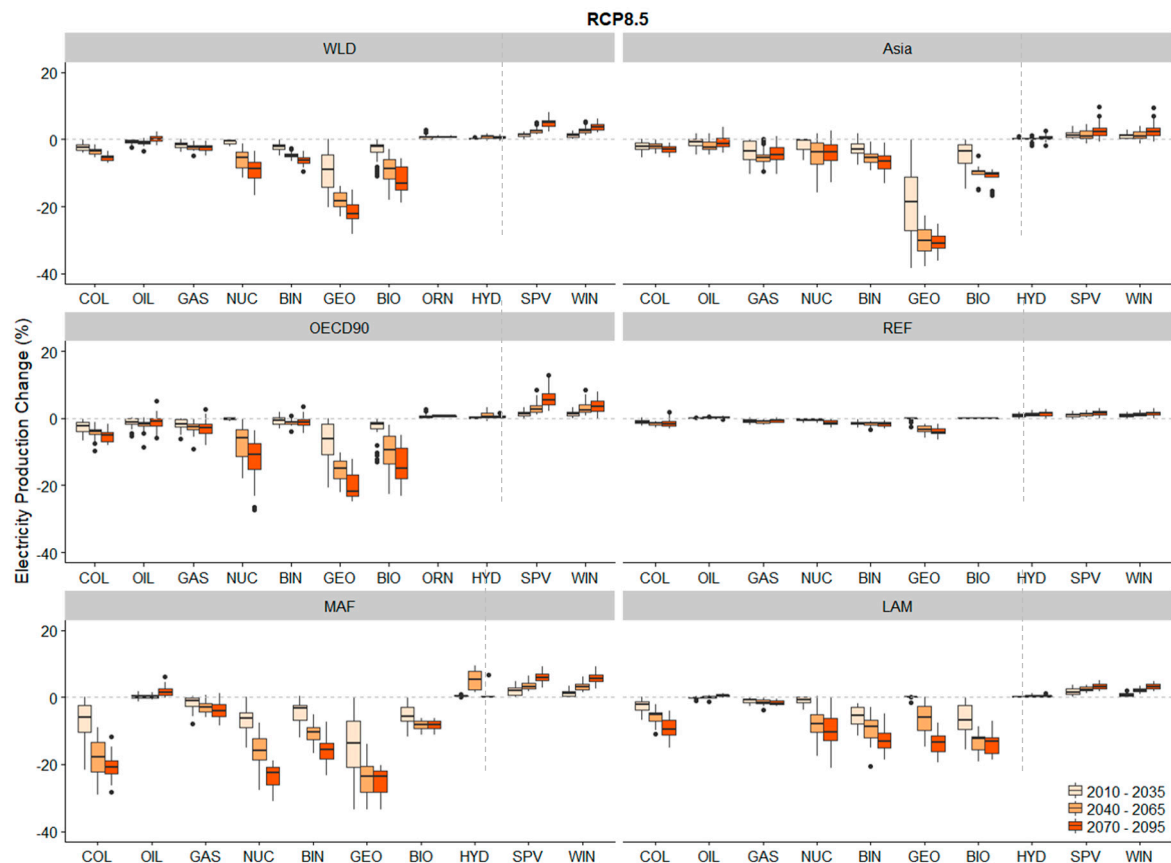
GAS (65.3 EJ yr<sup>-1</sup>), and NUC (48.6 EJ yr<sup>-1</sup>) were the main sources of thermolectric power, and HYD (36.8 EJ yr<sup>-1</sup>) was the primary source of non-thermolectric power. In Asia, COL electricity production displayed the most growth. In addition to COL, GAS and NUC grew substantially in OECD90, REF, and MAF. In LAM, HYD displayed the most growth, but it hit a ceiling because it reached the exploitable maximum hydropower potential in 2070–2095 (see Zhou et al. [20]). Non-thermal electricity production grew steadily, but the total production fell below that of thermal in all periods and regions except LAM in 2010–2035.



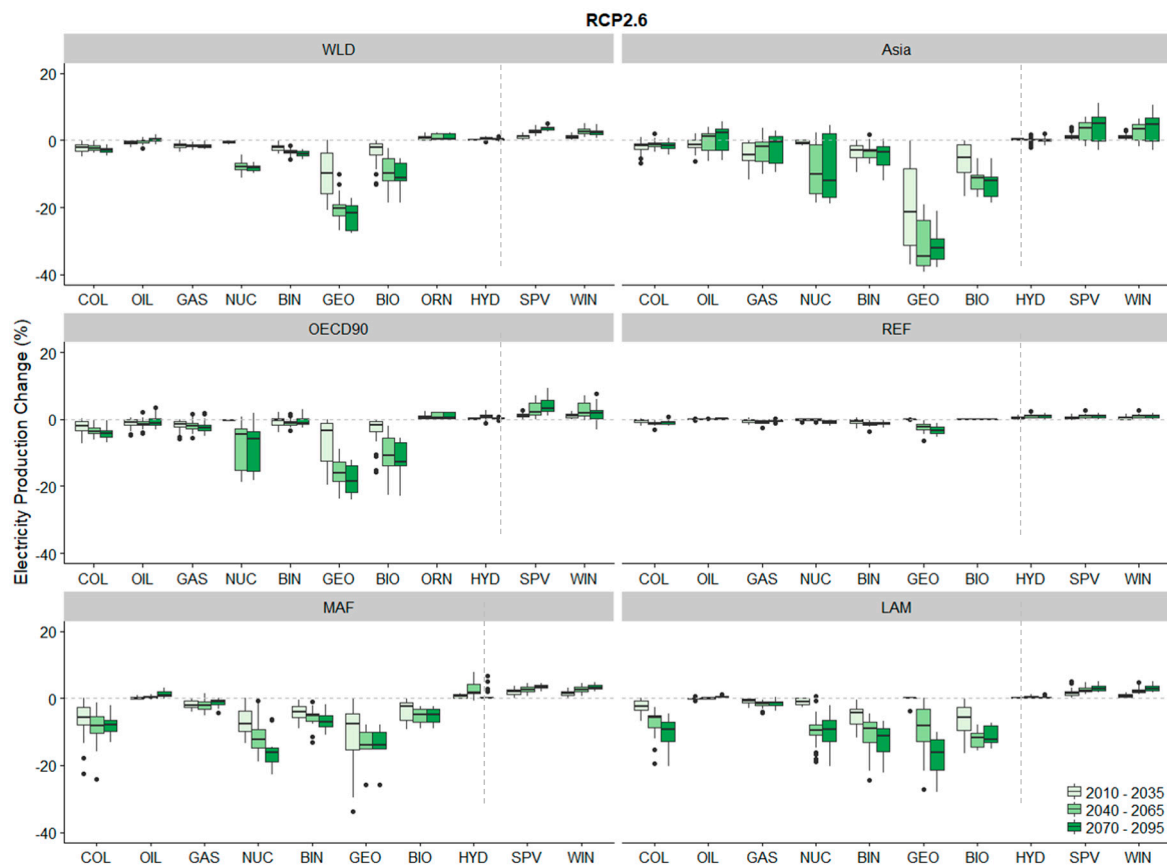
**Figure 3.** Projections of thermal and non-thermal electricity production in three periods, 2010–2035, 2040–2065, and 2070–2095, for the no climate change impacts (NoCC) run for the entire world (WLD) and for five regions (Asia, OECD90, REF, MAF and LAM; see Table S1). The box plots show the range within each period. The left and right of the dashed line are the thermolectric and non-thermolectric sectors, respectively.

Figure 4 shows the differences in electricity production between the RCP8.5 and NoCC runs (i.e., the impacts of RCP8.5 climate change on electricity production) in the three periods. In the WLD, there was a reduction in electricity production in all the thermal sectors due to climate change, whereas there was an increase in all the non-thermal sectors. The magnitude of the reduction in the WLD was  $-5.43\%$  for COL (median in 2070–2095),  $-8.84\%$  for NUC,  $-6.14\%$  for BIN,  $-22.1\%$  for GEO, and  $-13.0\%$  for BIO. In Asia, OECD90, and LAM, decreasing patterns similar to that observed for the WLD were apparent. Remarkable declines in GEO and NUC were projected in Asia and OECD90, respectively. In REF, all the sectors were marginally affected by climate change. MAF was the region that experienced the largest reduction due to climate change ( $-20.8\%$  for COL,  $-4.10\%$  for GAS,  $-22.4\%$  for NUC, and  $-15.5\%$  for BIN) and a substantial increase in non-thermal power ( $5.27\%$  for HYD,  $5.88\%$  for SPV, and  $5.67\%$  for WIN). Among the thermal power sectors, the difference in GEO was remarkable in all regions, although it played a marginal role in the total electricity supply because its overall contribution was marginal (Figure 3). In terms of electricity supply, the impacts on NUC had the largest effect, particularly in OECD90 and MAF.

Figure 5 shows the differences in electricity production between the RCP2.6 and NoCC runs in the three periods. Globally, the pattern of change was similar to that of the RCP8.5 run. The magnitude and variations (e.g., the range between the 25th and 75th percentiles) of change for the RCP2.6 run were smaller than those for the RCP8.5 run because both the magnitude and GCM uncertainty range of climate change impacts for the RCP2.6 run were smaller than those for the RCP8.5 run. Regionally, the uncertainty range in NUC was greater than that in the RCP8.5 run. This can be explained by two factors: (1) the stringent climate mitigation policy in RCP2.6 promotes the use of NUC and (2) the availability of cooling water differs substantially among the GCMs.



**Figure 4.** Differences in electricity production between the RCP2.6 and NoCC runs. The results of thermal and non-thermal sectors in three periods (2010–2035, 2040–2065, and 2070–2095) are shown. The range shows the variations in time and the differences among the five global climate models (GCMs).



**Figure 5.** Differences in electricity production between the RCP2.6 and NoCC runs. The results of thermal and non-thermal sectors in three periods (2010–2035, 2040–2065, and 2070–2095) are shown. The range shows the variations in time and the differences among the five global GCMs.

### 3.2. Economic Consequences of Climate Change

Figure 6 shows the changes in GDP due to cooling water insufficiency for the thermal power sector. We found that cooling water insufficiency decreased the GDP compared with the NoCC scenario for the world and five regions during the 21st century. Decreasing trends were consistently seen in all 10 experiments (i.e., five GCMs and two warming levels). We found that the global annual mean GDP loss was 0.07–0.08% in 2050 and 0.14–0.23% in 2100. The magnitude of the GDP loss varied among the regions. The largest reduction in GDP occurred in MAF. The magnitude of GDP loss was higher than the global mean throughout the century, with a value of 0.10–0.16% in 2050 and 0.27–0.57% in 2100. In contrast, there were minor GDP changes in LAM and Asia. The magnitude of GDP loss for the RCP2.6 (RCP8.5) run was 0.03% (0.03%) in 2050 and 0.06 (0.06%) in 2100 in LAM, and 0.06% (0.06%) in 2050 and 0.08 (0.09%) in 2100 in Asia. A moderate loss was projected in OECD90 and REF. The loss in the RCP2.6 (RCP8.5) run was 0.07 (0.09%) in 2050 and 0.12 (0.18%) in 2100 in OECD90, and 0.15 (0.11%) in 2050 and 0.12 (0.15%) in 2100 in REF.

The key drivers for the projected GDP loss were as follows. The first driver was an increase in the water requirement. The cooling water requirement grew rapidly alongside the growth in electricity demand and with a shift in thermal power plant cooling systems from once-through flow to a closed loop [10]. The water requirement for other sectors, such as agriculture, manufacturing, and household use, also grew rapidly, particularly in developing regions such as Asia, LAM, and MAF. Subsequent water competition among sectors and regions caused water insufficiency. The second factor was the changing climate. Climate change intensified the contrast between wet and dry periods, with a consequent decrease in water availability, particularly in dry periods [10]. Both the increased water requirement and decreased water availability resulted in a decline in CWS. The third driver

was a reduction in the capital productivity of the thermal power sector, which was transferred from cooling water insufficiency (see Methods). A reduction in capital productivity reduces the price competitiveness of thermoelectric power compared to non-thermal power; hence, negative and positive shifts in the thermal and non-thermal power sectors were observed (Figures 4 and 5). Due to the limitations in resources and the efficiency of non-thermal electricity production, the overall economic efficiencies of the RCP2.6 and RCP8.5 runs fell below that of the NoCC run. The fourth driver was dependency on thermoelectric power and its dominance in value added among industries in the regions in question. For example, electricity in LAM was predominantly supplied by non-thermal hydropower (Figure 3); hence, the GDP loss was marginal (Figure 5d). Because the GDP of the power production sector was marginal (substantial) in Asia (REF), the GDP loss was minor (substantial).

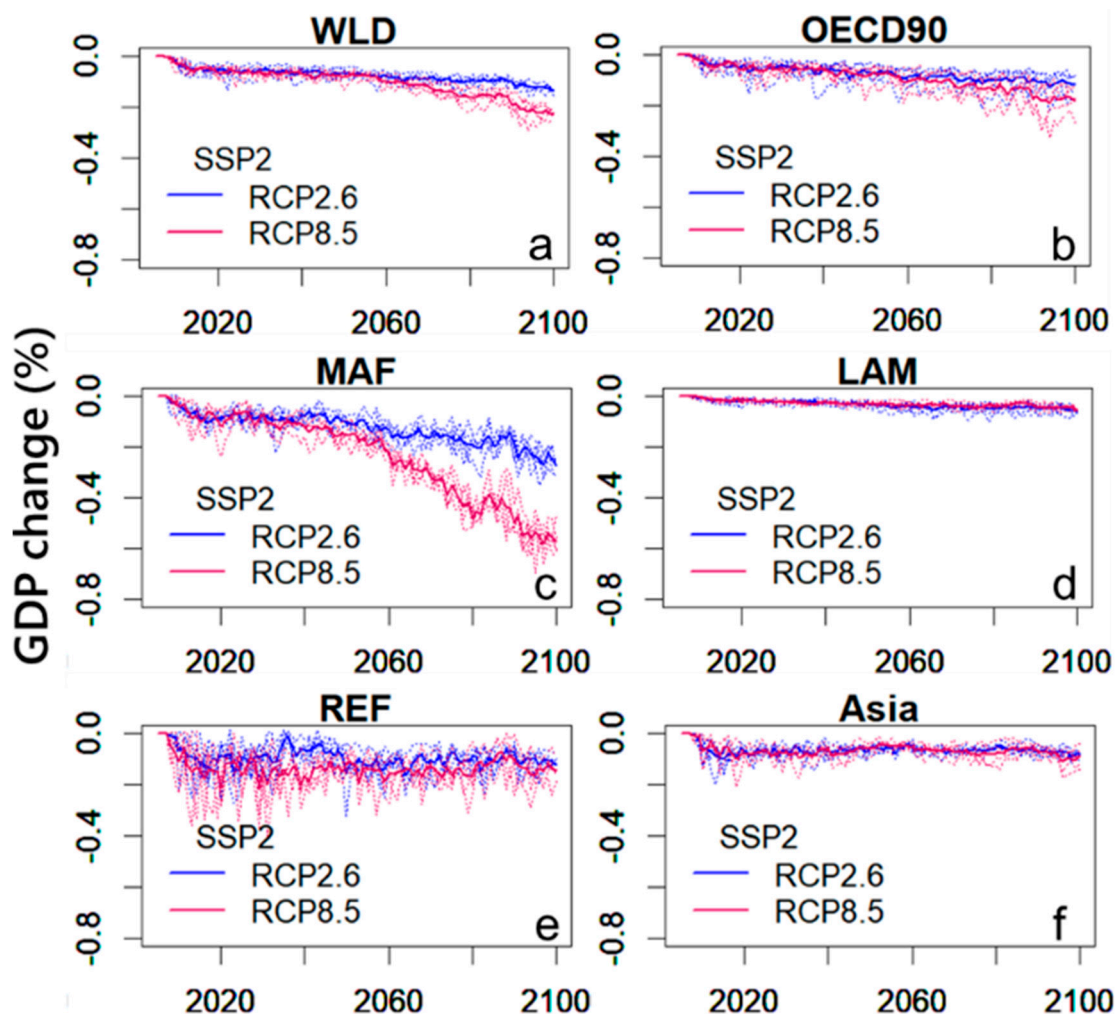


**Figure 6.** Differences in gross domestic product (GDP) between the RCP2.6 and NoCC runs (blue) and the RCP8.5 and NoCC runs (pink) for (a) the WLD, (b) OECD90, (c) MAF, (d) LAM, (e) REF, and (f) Asia (see Table S1). The thin dotted and bold solid lines show the results using the cooling water insufficiency projected by five individual GCMs and the ensemble mean, respectively.

### 3.3. Decomposition Analysis of Economic Changes

To identify sector-wise economic impacts, the changes in value added were examined for six aggregated industrial sectors for the RCP2.6 and RCP8.5 runs in comparison with the NoCC run (Figure 7). As commonly seen in all regions, PWR and SER were the sectors with a remarkable reduction in value added. In LAM, ENE (447.0 million USD in 2070–2095 for the RCP8.5 run) had a clear increase in value added. In MAF, the largest reduction in value added was found for SER.

The reduction was doubled in the RCP8.5 run (−4772 million USD) compared to the RCP2.6 run (−2177 million USD). The remarkable change in GDP in MAF (Figure 6c) was mainly attributed to the reduction in economic activity in SER. In OECD90, the reductions in value added for SER and PWR were −4110 and −6451 million USD, respectively, for the RCP8.5 run in 2070–2095, which was the largest reduction among all the results. In REF, in addition to SER and PWR, the reduction in value added for MAN was also large.

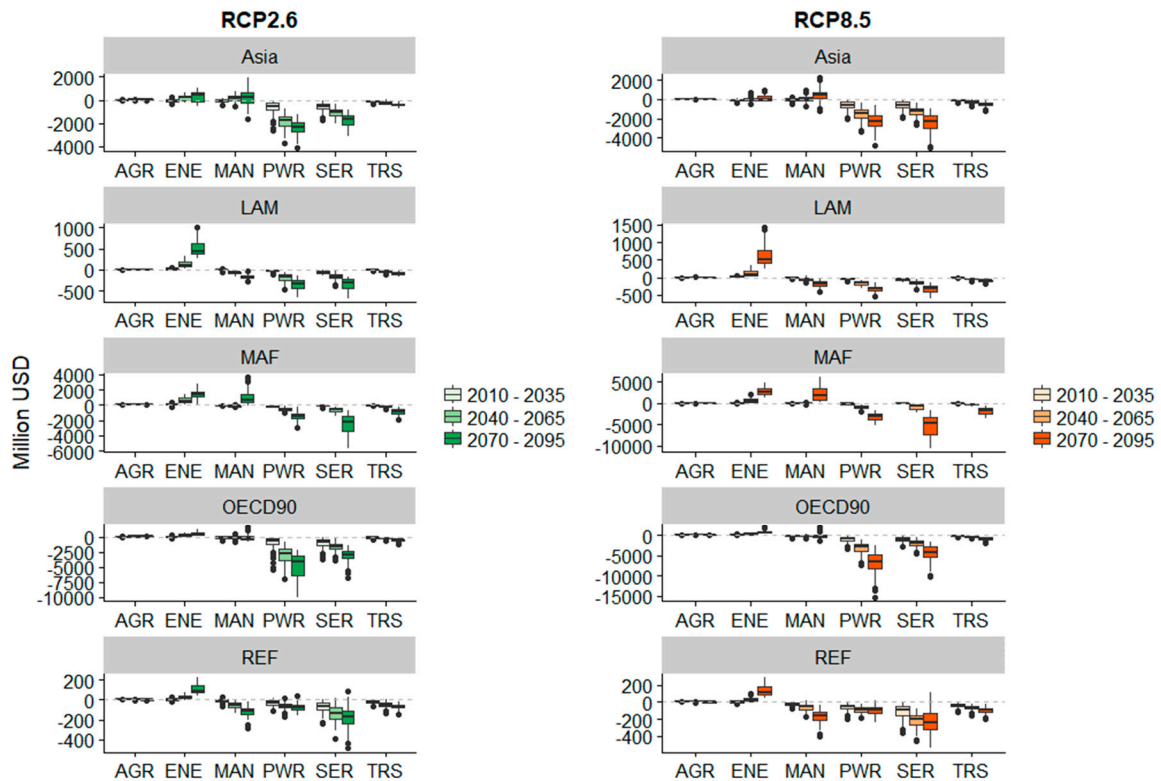


**Figure 7.** Industry-wise change in value added for the RCP2.6 and RCP8.5 runs. AGR, agriculture; MAN, manufacturing and construction; ENE, energy extraction; SER, service; PWR, power; TRS, transport and communication.

#### 4. Conclusions

This study quantified the global economic consequences of the impacts of climate change on the thermal power sector by a two-way coupling of a physical hydrological model and an economic model. The two models were linked by transforming the CWS simulated by the hydrological model into the capital productivity of thermoelectric sectors in the economic model. A reduction in the availability of cooling water suppressed thermoelectric power production. Power generation by COL and NUC showed the largest declines due to cooling water insufficiency among the three predominant power sources (the other being GAS). MAF was the region with the largest decrease, approximately 20% in 2070–2095 for the RCP8.5 run. The change in thermoelectric power production propagated into the global economy. The ensemble-mean results showed that the global GDP loss due to cooling water insufficiency in the thermal power sector was −0.12% (−0.21%) in the RCP2.6 (RCP8.5) run. Among the five regions, the largest GDP loss of −0.27% (−0.57%) was observed in MAF. Medium-scale losses of −0.12% (−0.18%) and −0.12% (−0.14%) were found in OECD90 and REF, respectively. The smallest losses of −0.06% (−0.05%) and −0.08% (−0.09%) were found in LAM and Asia, respectively. A reduction in value added in the power sector was found in all regions. The largest reductions were found in OECD90 and MAF in terms of the absolute monetary value and the percentage of regional GDP, respectively. The largest reduction in value added was found in the service sector, which significantly influenced the regional GDP.

To the best of our knowledge, this is the first study to quantify the physical impacts of climate change on the thermal power sector by coupling a physical hydrological model and an economic model at the global scale. The regional and sectorial variations in response to cooling water shortage highlight the importance of incorporating geographical and sectorial details into physical hydrological and economic models. There are multiple ways to interpret the economic consequences. When compared with other sectors that face economic impacts from climate change, the percentage GDP decreases were found to be comparable to the losses in other sectors due to energy demand [21], human health due to undernourishment [22], and floods [23]. This implies that cooling water insufficiency is non-negligible and should be considered as one of the threats induced by climate change. Climate change mitigation actions can negate these effects in two ways: (1) by reducing climate change itself and (2) by changing the power generation system to rely less on thermoelectricity (e.g., such as solar and wind), which can be interpreted as an adaptive measure (e.g., van Vliet et al. [6]). This duality of climate change mitigation in the context of saving cooling water should be seriously considered by policy makers as one of the benefits of climate change mitigation.

**Supplementary Materials:** The following are available online at <http://www.mdpi.com/1996-1073/11/10/2686/s1>. Table S1: Regional classification and Table S2: Sectorial classification.

**Author Contributions:** N.H. and S.F. conceived of and designed the experiments; Q.Z., N.H. and S.F. performed the experiments; Q.Z., N.H. and S.F. analyzed the data and wrote the first draft.

**Funding:** This work was supported by the Environment Research and Technology Development Fund (S-14) of Environmental Restoration and Conservation Agency, Japan.

**Conflicts of Interest:** The authors declare no conflict of interest.

## References

1. International Energy Agency (IEA). *Key World Energy Statistics 2017*; International Energy Agency: Paris, France, 2017; p. 95.
2. Kenny, J.F.; Barber, N.L.; Hutson, S.S.; Linsey, K.S.; Lovelace, J.K.; Maupin, M.A. *Estimated Use of Water in the United States in 2005*; U.S. Geological Survey Circular 1344; U.S. Geological Survey: Reston, VA, USA, 2009; p. 52.
3. European Commission. Eurostat. Available online: <https://ec.europa.eu/eurostat> (accessed on 1 September 2018).
4. Hanasaki, N.; Fujimori, S.; Yamamoto, T.; Yoshikawa, S.; Masaki, Y.; Hijioka, Y.; Kainuma, M.; Kanamori, Y.; Masui, T.; Takahashi, K.; et al. A global water scarcity assessment under shared socio-economic pathways—Part 1: Water use. *Hydrol. Earth Syst. Sci.* **2013**, *17*, 2375–2391. [[CrossRef](#)]
5. Van Vliet, M.T.H.; Yearsley, J.R.; Ludwig, F.; Vogele, S.; Lettenmaier, D.P.; Kabat, P. Vulnerability of us and european electricity supply to climate change. *Nat. Clim. Chang.* **2012**, *2*, 676–681. [[CrossRef](#)]
6. Van Vliet, M.T.H.; Wiberg, D.; Leduc, S.; Riahi, K. Power-generation system vulnerability and adaptation to changes in climate and water resources. *Nat. Clim. Chang.* **2016**, *6*, 375–380. [[CrossRef](#)]
7. Boogert, A.; Dupont, D. The nature of supply side effects on electricity prices: The impact of water temperature. *Econ. Lett.* **2005**, *88*, 121–125. [[CrossRef](#)]
8. Bartos, M.D.; Chester, M.V. Impacts of climate change on electric power supply in the western United States. *Nat. Clim. Chang.* **2015**, *5*, 748–752. [[CrossRef](#)]
9. Miara, A.; Macknick, J.E.; Vörösmarty, C.J.; Tidwell, V.C.; Newmark, R.; Fekete, B. Climate and water resource change impacts and adaptation potential for us power supply. *Nat. Clim. Chang.* **2017**, *7*, 793–798. [[CrossRef](#)]
10. Zhou, Q.; Hanasaki, N.; Fujimori, S.; Yoshikawa, S.; Kanae, S.; Okadera, T. Cooling water sufficiency in a warming world: Projection using an integrated assessment model and a global hydrological model. *Water* **2018**, *10*, 872. [[CrossRef](#)]
11. Kyle, P.; Davies, E.G.R.; Dooley, J.J.; Smith, S.J.; Clarke, L.E.; Edmonds, J.A.; Hejazi, M. Influence of climate change mitigation technology on global demands of water for electricity generation. *Int. J. Greenh. Gas Control* **2013**, *13*, 112–123. [[CrossRef](#)]
12. Fujimori, S.; Hanasaki, N.; Masui, T. Projections of industrial water withdrawal under shared socioeconomic pathways and climate mitigation scenarios. *Sustain. Sci.* **2017**, *12*, 275–292. [[CrossRef](#)] [[PubMed](#)]

13. Ando, N.; Yoshikawa, S.; Fujimori, S.; Kanae, S. Long-term projections of global water use for electricity generation under the shared socioeconomic pathways and climate mitigation scenarios. *Hydrol. Earth Syst. Sci.* **2017**, *2017*, 1–25. [[CrossRef](#)]
14. Fujimori, S.; Hasegawa, T.; Masui, T.; Takahashi, K.; Herran, D.S.; Dai, H.; Hijioka, Y.; Kainuma, M. Ssp3: Aim implementation of shared socioeconomic pathways. *Glob. Environ. Chang.* **2017**, *42*, 268–283. [[CrossRef](#)]
15. Hanasaki, N.; Kanae, S.; Oki, T.; Masuda, K.; Motoya, K.; Shirakawa, N.; Shen, Y.; Tanaka, K. An integrated model for the assessment of global water resources—Part 1: Model description and input meteorological forcing. *Hydrol. Earth Syst. Sci.* **2008**, *12*, 1007–1025. [[CrossRef](#)]
16. Hanasaki, N.; Kanae, S.; Oki, T.; Masuda, K.; Motoya, K.; Shirakawa, N.; Shen, Y.; Tanaka, K. An integrated model for the assessment of global water resources—Part 2: Applications and assessments. *Hydrol. Earth Syst. Sci.* **2008**, *12*, 1027–1037. [[CrossRef](#)]
17. Fujimori, S.; Tu, T.T.; Masui, T.; Matsuoka, Y. *AIM/CGE [Basic] Manual; Center for Social and Environmental Systems Research; National Institute for Environmental Studies: Tsukuba, Japan, 2012; p. 74.*
18. Lofgren, H.; Harris, R.L.; Robinson, S. *A Standard Computable General Equilibrium (CGE) Model in GAMS; International Food Policy Research Institute: Washington, DC, USA, 2002; p. 69.*
19. O'Neill, B.; Kriegler, E.; Riahi, K.; Ebi, K.; Hallegatte, S.; Carter, T.; Mathur, R.; van Vuuren, D. A new scenario framework for climate change research: The concept of shared socioeconomic pathways. *Clim. Chang.* **2014**, *122*, 387–400. [[CrossRef](#)]
20. Zhou, Q.; Hanasaki, N.; Fujimori, S.; Masaki, Y.; Hijioka, Y. Economic consequences of global climate change and mitigation on future hydropower generation. *Clim. Chang.* **2018**, *147*, 77–90. [[CrossRef](#)]
21. Hasegawa, T.; Park, C.; Fujimori, S.; Takahashi, K.; Hijioka, Y.; Masui, T. Quantifying the economic impact of changes in energy demand for space heating and cooling systems under varying climatic scenarios. *Palgrave Commun.* **2016**, *2*, 16013. [[CrossRef](#)]
22. Hasegawa, T.; Fujimori, S.; Takahashi, K.; Yokohata, T.; Masui, T. Economic implications of climate change impacts on human health through undernourishment. *Clim. Chang.* **2016**, *136*, 189–202. [[CrossRef](#)]
23. Dottori, F.; Szewczyk, W.; Ciscar, J.-C.; Zhao, F.; Alfieri, L.; Hirabayashi, Y.; Bianchi, A.; Mongelli, I.; Frieler, K.; Betts, R.A.; et al. Increased human and economic losses from river flooding with anthropogenic warming. *Nat. Clim. Chang.* **2018**, *8*, 781–786. [[CrossRef](#)]



© 2018 by the authors. Licensee MDPI, Basel, Switzerland. This article is an open access article distributed under the terms and conditions of the Creative Commons Attribution (CC BY) license (<http://creativecommons.org/licenses/by/4.0/>).